Available online at www.sciencedirect.com
ScienceDirect
Polymer 48 (2007) 7476–7483
polymer
www.elsevier.com/locate/polymer

Polybutadiene/poly(ethylene oxide) based IPNs, Part II: Mechanical modelling and $LiClO_4$ loading as tools for IPN morphology investigation

Catherine Gauthier [a], Cédric Plesse [b], Frédéric Vidal [b], Jean-Marc Pelletier [a], Claude Chevrot [b], Dominique Teyssié [b,*]

[a] *MATEIS, INSA Lyon, Bat. B. Pascal, 69621 Villeurbanne, France*
[b] *Laboratoire de Physico-chimie des Polymères et des Interfaces, Université Cergy-Pontoise, 5 mail Gay-Lussac, 95031 Cergy-Pontoise Cedex, France*

Received 6 April 2007; received in revised form 10 October 2007; accepted 12 October 2007

Abstract

Interpenetrating polymer networks (IPNs) combining polybutadiene (PB) and poly(ethylene oxide) (PEO) show very close α relaxations leading to a partially resolved signal as determined by DMA. Nevertheless it is shown in this paper, in complement to part I, that it is still possible to get a better insight into the material morphology through two different approaches. First DMA experimental data are compared with theoretical predictions obtained from mechanical coupling models (Christensen and Lo and Budiansky approaches). Second, it is shown that full splitting of DMA signals can be induced providing that $LiClO_4$ is introduced in polybutadiene/poly(ethylene oxide) IPNs. Indeed the Li^+ cation has a particular affinity for the ethylene oxide segments in the PEO network. IPN morphologies are then discussed much more accurately according to $LiClO_4$ loaded IPN mechanical behaviour. This concept could be usefully generalized to other types of polymers IPN associations as long as a selective complexation agent for one of the partner networks can be found that selectively modifies one particular property of this partner network.

Keywords: Interpenetrating polymer networks; Dynamic mechanical properties; Hydroxytelechelic polybutadiene

1. Introduction

Interpenetrating polymer networks (IPNs) are materials where both components (and sometimes one only in semi-IPNs) are cross-linked according to simultaneous or sequential polymerisation processes. They have been investigated extensively, as evidenced by a number of reviews and monographs [1–5]. The phrase ''interpenetrating polymer network'' was first coined by Millar in a study concerning ion-exchange materials containing sulfonated polystyrene [6,7]. Millar postulated that the two different networks intermeshed on a molecular level even though there was no evidence for this precise morphology. Actually, due to low entropy and positive heats of mixing, most IPNs phases separate to variable extent, although much less than conventional blends do. Indeed, the formation of network architectures restricts the domain size significantly in IPNs. Miscibility in multicomponent polymeric systems, even more in binary polymer blends, has been extensively studied [8–13]. In an immiscible polymer blend, the polymer phases often separate into domains larger than a few micrometers with poor interphase, leading to an opaque appearance. Conversely, the domain sizes in IPNs are typically around 30–100 nm, which result in optical transparency and in extended interface between the two components [4]. The specific mechanical and optical properties of IPNs are thus associated with a specific morphology

* Corresponding author. Tel.: +33 1 34 25 70 50; fax: +33 1 34 25 70 70.
E-mail address: dominique.teyssie@chim.u-cergy.fr (D. Teyssié).

0032-3861/$ - see front matter © 2007 Elsevier Ltd. All rights reserved.
doi:10.1016/j.polymer.2007.10.035

developed during the synthesis [14,15]. For instance, each network phase continuity affects penetrant diffusion, swellability, tensile strength, and modulus. The continuity is affected by many of the variables that control domain sizes, such as the rate of each polymerisation process, the crosslink density and the amount of each component. The first network formed is assumed to be continuous in space but many IPNs show dual-phase continuity, which means that both phases are continuous throughout the macroscopic sample [2]. It is often postulated that continuity is only possible if significant amounts of each component are present in the IPN, i.e. around a 1/1 weight ratio [1,2].

IPN applications extend in fields such as semi-permeable membranes, ion-exchange resins, damping, toughening or impact-modifiers [1,2]. IPNs can be designed to absorb mechanical energy if one component is a rubbery material and the other is a rigid, glassy material at room temperature. When these two materials interpenetrate, an interphase is generated with a glass transition temperature between those of both components. In such a case, energy absorption may be enhanced over a large temperature range leading to high damping characteristics. IPNs also offer a convenient method for the preparation of solid polymer electrolytes (SPEs) which is the particular application which was sought for the IPNs described in this paper [16–19].

In the present work, IPNs combining poly(ethylene oxide)/polybutadiene (PEO/PB) were prepared by free radical copolymerization of poly(ethylene glycol) dimethacrylate and methacrylate, and polyaddition of α,ω hydroxy functionalized polybutadiene. The kinetics of PEO and PB networks and IPN formations were investigated by FT-NIR and the results were published previously [20]. However, in this former work, DMA data showed that the α-relaxation temperatures of the two networks are very close to each other, i.e. $T_\alpha = -44$ °C and $T_\alpha = -64$ °C for PEO and PB, respectively, unfortunately leading to partially resolved signals.

The present paper proposes two additional approaches based on DMA investigation of the synthesized IPNs which enlighten a possibly more accurate relation to their morphology. The first approach derives from mechanical coupling models. Viscoelastic data generally are either presented as shear modulus (G^*) or tensile modulus (E^*) depending on the applied deformation mode. In this work, measurements were performed in both tensile and torsion modes and the comparison of the two sets of results shows that both modes lead to comparable results. Subsequently experimental data on PEO/PB IPNs were compared to theoretical predictions (using Christensen and Lo and Budiansky expressions) in order to get a better insight into the morphology.

Second, advantage was taken from the fact that an increase of the α-relaxation temperature in a lithium-added PEO system is commonly observed, due to the dipole cation interactions between the polyether and Li^+ [21], in other words physical cross-linking. Thus a lithium salt was inserted in the material in order to increase the difference between the α-relaxation temperatures of the PB and the PEO networks. It was hoped and it turned out that this procedure induces a separation of the PEO and PB T_α relaxations allowing an accurate analysis of the influence of the PEO/PB relative weight proportions in the IPN on the viscoelastic response and on the morphology.

2. Experimental

2.1. Materials

Poly(ethylene glycol) dimethacrylate (PEGDM, $M_n = 875$ g mol^{-1}) (Aldrich), poly(ethylene glycol) methyl ether methacrylate (PEGM, $M_n = 475$ g mol^{-1}) (Aldrich), hydroxyl end-functionalized polybutadiene – (HTPB, $M_n = 2800$ g mol^{-1}, alcohol functionality $f_{OH} = 2.4$) (Cray Valley), dicyclohexylperoxydicarbonate (DCPD) initiator (Groupe Arnaud), Desmodur® N3300 (pluri-NCO cross-linker, 5.2×10^{-3} mol of NCO per gram of Desmodur) (Bayer), lithium perchlorate (Aldrich) and dibutyltindilaurate (95%) (DBTDL) (Aldrich) were used without further purification. Toluene (VWR) was distilled before use.

2.2. Synthesis

2.2.1. Preparation of single networks

PEO single networks were prepared as following: 0.75 g PEGM, 0.25 g PEGDM, 22 mg DCPD (2.2 wt% with respect to the sum of methacrylate oligomers weight) were stirred together under argon atmosphere for 30 min at room temperature. The mixture was then poured into a mould made from two glass plates clamped together and sealed with a 250 or 500 μm thick Teflon® gasket. The mould was then kept at 50 °C for 3 h. The sample was then cured for 1 h at 80 °C.

HTPB single networks were prepared by dissolving 1 g HTPB into 1 mL toluene. To this solution 0.18 g Desmodur® N3300 ([NCO]/[OH] = 1.1) and 32 μL DBTDL ([DBTDL]/[OH] = 0.06) (cross-linker and catalyst for the HTPB network formation, respectively) were added. The mixture was then poured into a mould made from two glass plates clamped together and sealed with a 250 or 500 μm thick Teflon® gasket. The mould was then kept at 50 °C for 3 h. The sample was finally cured for 1 h at 80 °C and dried for 8 h at 50 °C under vacuum.

2.2.2. IPN preparation

DCPD was used for methacrylate radical initiation of PEGDM and PEGM methacrylate functions, while Desmodur® N3300 was the cross-linker for HTPB and DBTDL the catalyst for the reaction between NCO and OH functions. The given amounts of PEGDM, PEGM, HTPB were poured as such into a flask. In all IPN preparations reported in this study, PEGM and PEGDM were introduced in a three to one weight ratio corresponding to 75 wt% PEGM and 25 wt% PEGDM into the PEO network. Desmodur® was then added to the mixture ([NCO]/[OH] = 1.1) as well as the DCPD initiator (2.2 wt% with respect to the sum of methacrylate oligomers weight). The minimum volume of toluene (typically 1 mL for a total weight of 1 g of PEGDM, PEGM and HTPB) is then added to ensure the homogeneity of the mixture. The obtained solution was stirred under

argon atmosphere for 30 min, and DBTDL catalyst was then added ([DBTDL]/[OH] = 0.06). The mixture was poured into a mould made from two glass plates clamped together and sealed with a 250 or 500 μm thick Teflon® gasket. This mould was then kept at 50 °C for 3 h. The sample was then post-cured for 1 h at 80 °C and dried for 8 h at 50 °C under vacuum.

In the following text ($X/(100-X)$) IPN stands for an IPN obtained from X wt% PEGM/PEGDM and $(1-X)$ wt% HTPB in the starting mixture. The detailed synthesis of the materials and corresponding kinetics of the formation of the individual networks and IPNs (studied by Fourier transform spectroscopy) are reported elsewhere [20].

2.2.3. IPN characterization

In order to examine the $LiClO_4$ loading capacity, PEO/PB IPN films with accurately known weights are immersed in aqueous $LiClO_4$ solution (1 mol L^{-1}) at room temperature. Samples are dried overnight at 50 °C under vacuum and carefully weighted.

Viscoelastic behaviour is generally investigated by dynamic tests that measure the response of the material to a sinusoidal stress. In this work, measurements are performed both in tensile and torsion modes. Torsion tests are conducted, thanks to a home made pendulum on rectangular specimens of 12 mm length, 4 mm width and 0.5 mm thickness. Experiments are made at a fixed frequency (0.1 or 1 Hz) with a constant heating rate (1 K min^{-1}) between −170 and 50 °C. The set-up provides the storage and the loss components G' and G'', respectively, and the loss factor $\tan\delta = G''/G'$ of the complex shear modulus G^*. Shear modulus was normalized at 1 GPa at −170 °C. Tensile measurements are performed using Q800 apparatus (TA instruments). In that case, samples' dimensions are $15 \times 8 \times 0.5$ mm^3 and the applied strain is in the range 0.05–0.07%. In tensile mode, DMA experiments are carried out from −100 to 50 °C with a heating rate of 2 K min^{-1} and a complex tensile modulus E^* ($E' + jE''$) is obtained. The viscoelastic behaviour of samples is investigated in tensile mode.

3. Results and discussion

3.1. Dynamic mechanical characterization of PEO/PB IPNs and mechanical modelling

In a previous paper [20] a series of PEO/PB IPNs were prepared in order to examine the effect of varying the relative PEO weight proportion (80, 60, 50, 40 and 20 wt%) on the material morphology as investigated by DMA. However, on the sole DMA and TEM basis it was only possible to conclude that the 80/20 PEO/PB IPN assumes a dual-phase continuity morphology. For the IPNs with other composition values (60/40–20/80) a different strategy had to be adopted in order to assess precise morphology.

Assuming as it is generally observed, that torsion mode DMA measurements are more sensitive, due to the fact that no predeformation of the sample is necessary, the measurements in tensile mode were compared with measurements in torsion mode for single networks.

Shear complex modulus G^* is obtained directly from torsion measurements. In order to compare experiments performed using either shear or tensile stress, values of E^* have been transformed into G^* values. Eq. (1) gives the relationships between the different elastic moduli: E (Young's modulus), G (shear modulus), K (bulk modulus) and the Poisson coefficient (ν).

$$G = \frac{E}{2(1+\nu)} \quad \text{and} \quad G = \frac{3KE}{9K-E} \tag{1}$$

Owing to the corresponding principle of Hashin [22], these expressions can be applied to complex modulus. Then, assuming that the Poisson coefficient is a true real, expression (1) can be used to directly calculate either G' or G''. For polymers, the variation of K with temperature is known to be negligible compared to those of other elastic moduli. The Poisson coefficient ν is about 0.32 in the glassy state. This value is used at $T = -100$ °C to estimate the bulk modulus. Then, the values of G' and G'' can be deduced from E' and E'' at any temperature. This allows to plot on a same graph both the values of G' measured directly in torsion mode and the values of G' calculated from E', i.e. from tensile measurements. Fig. 1A and B shows the results for PB and PEO single networks studied in torsion and tensile modes with a fixed frequency (1 Hz) as a function of temperature. For PB network (Fig. 1A), both series of data are in good agreement, despite the difference in

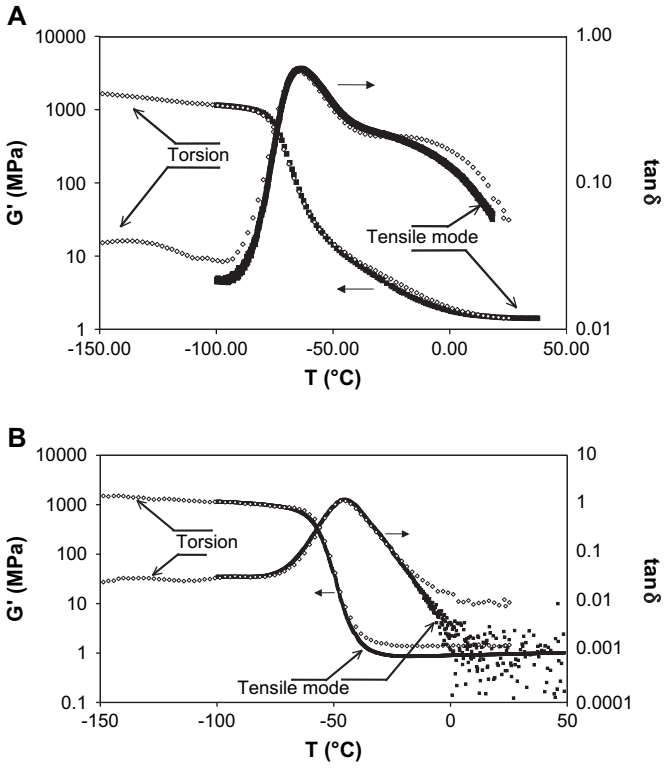

Fig. 1. Viscoelastic properties versus temperature (measured in torsion and in tensile modes at 1 Hz): (A) for PB network and (B): for POE network.

geometry and oven thermal characteristics of the two devices. Some discrepancies appear in the case of PEO (Fig. 1b), mainly in the rubbery plateau: the modulus calculated from tensile measurements is lower than that from torsion data. At the same time, the scattering of tan δ values indicates that the tensile measurements are probably performed near the limit of sensitivity of the apparatus above 0 °C in particular (i.e. below 10^{-3} N). Consequently, further comparison with theoretical models will only concern data obtained from torsion measurements. Thereafter all IPNs were investigated in torsion mode and the experimental data were compared with theoretical prediction. The comparison was then discussed in terms of IPN morphology.

The effects of the introduction of PB in the PEO network on the G' and tan δ curves for the different IPNs are presented in Fig. 2. Values of G' have been normalized using the value at −100 °C (in the glassy plateau). The main evolutions concerning the relaxation processes have been discussed in a previous publication [20]. To go further, the loss factor evolution can be analyzed by considering the sub-T_g relaxations (Fig. 3). As the secondary relaxations of polymers are associated with localized mobility, the presence of all the different relaxation processes associated with both components is expected in the IPNs. If we consider the loss factor in the sub-T_g temperature range, it is not possible to separate β relaxation of PB and γ relaxation of PEO (since temperatures are the same). However, the β relaxation of PEO is clearly detected in IPNs and its

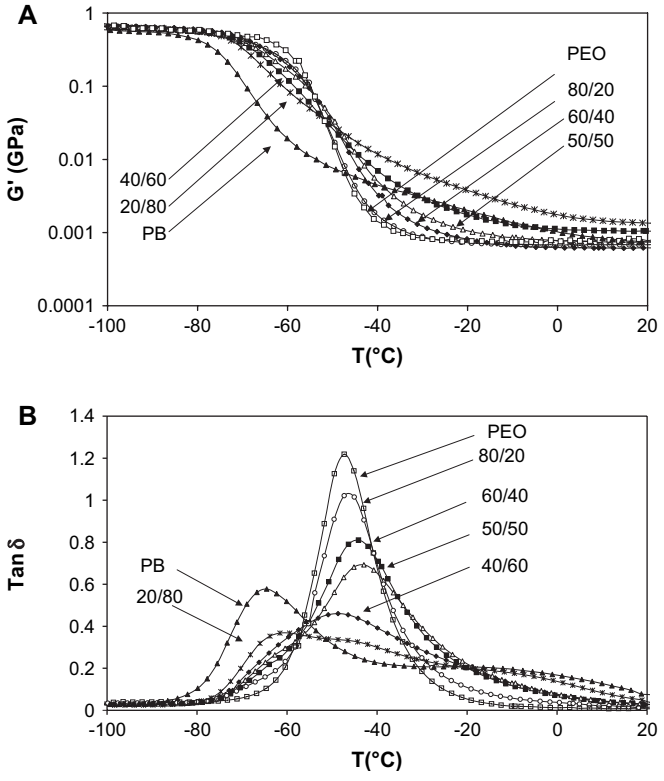

Fig. 2. Viscoelastic properties versus temperature for PEO/PB ($X/100 - X$) IPNs (measured in torsion at 0.1 Hz): (A) storage modulus and (B) loss factor (linear scale).

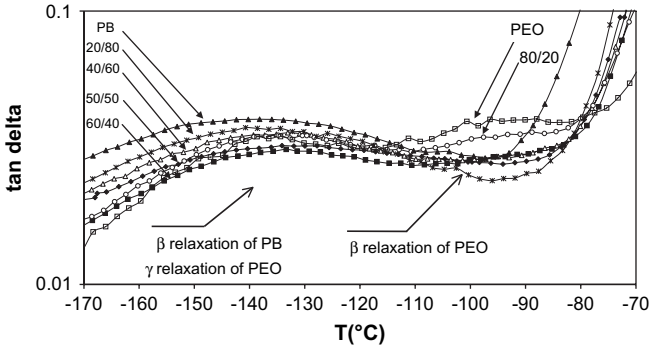

Fig. 3. Loss factor (tan δ) versus temperature in the sub-T_g range for PEO/PB ($X/100 - X$) IPNs (logarithmic scale).

amplitude increases with the PEO amount. Due to the presence of the PB α relaxation at temperature just above, it is difficult to quantitatively determine the amplitude of this β relaxation peak without further deconvolution. Conversely, the magnitude of the two α relaxation peaks have been measured for the different IPNs and plotted versus PEO content in Fig. 4. It can be observed that the peak amplitudes follow a mixture rule, i.e. depend mainly on the composition. Hence, it is difficult to conclude directly on the morphology of IPNs from DMA results. This is the reason why it was hoped that useful information could be expected from the comparison of these data with mechanical modelling.

From the point of view of the mechanics, composites, blends and even IPNs can be considered as heterogeneous materials. The models generally take into account the properties and the volume fractions of each phase and assume a given morphology (phase repartition, stress or strain continuity) but in most of cases, the size of the domains is not a considered parameter. Three general kinds of coupling models can be distinguished: (i) boundary models, based on variational methods, which define the extreme elastic behaviours of composites (e.g., Voigt and Reuss bounds), (ii) phenomenological approaches (e.g., series-parallel model of Takayanagi et al. [23]) introducing one or more adjustable parameters and (iii) micro-mechanical modelling, established on the definition of a "representative volume element" (RVE), like for instance selfconsistent estimations (3-phase model by Christensen and Lo [24], *n*-phase model by Herve and Zaoui [25]). In this work, use was made of two different models to reproduce either a phase separated morphology or a co-continuous network. Christensen and Lo expression assumes a morphology made of inclusions in a continuous matrix with PB (noted C−L_{PB}) or PEO (noted C−L_{PEO}) as the continuous phase. The model of Budiansky [26] which suits for phase inversion was also applied. To compare the different modelling approaches with DMA results, calculations are often applied only to the storage modulus, either in the glassy or in the rubbery plateau and plotted versus composition. This is appropriate only as far as the G'' modulus is negligible compared to the storage one G'. In the other case, i.e. in the main relaxation temperature domain, analytical formalism of the mechanical model has to be applied on complex modulus, thanks to the

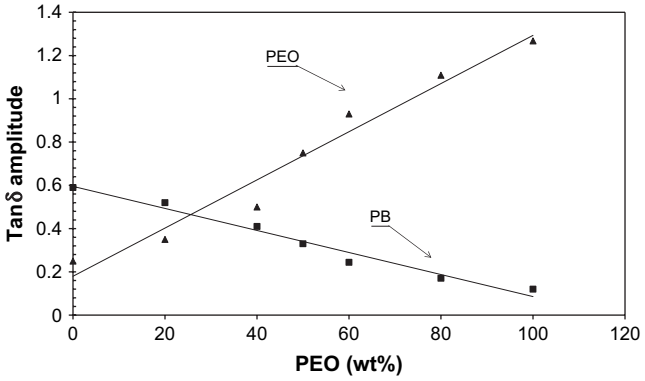

Fig. 4. Loss factor (tan δ) amplitude of relaxation peaks versus PEO content for PEO/PB IPNs: (■) α relaxation of PB, (▲) α relaxation of PEO.

corresponding principle of Hashin [22]. At each temperature, the complex modulus of the biphasic material is calculated from the experimental complex modulus of the constitutive phases. That allows to plot the evolution of G', G'' and loss factor of the heterogeneous sample versus temperature, and is often used in the field of polymers blends or nanocomposites [27,28].

First the results in the case of large PEO amount will be discussed (i.e. 80/20 IPN). Fig. 5 compares the G' and loss factor data with the different calculated results. It appears that, for this composition, calculations with Budiansky expression are superimposed with Christensen and Lo prediction when PEO is assumed to be the continuous phase ($C-L_{PEO}$). Concerning the modulus, the three expressions give a good fit in the range [−100 to −40 °C]. However, for temperatures above −40 °C, i.e. in the rubbery plateau, none of the modelling prediction fits the modulus data in a satisfactory way: the IPN moduli are found to be lower than that of the softer phase, i.e. PEO. One reason that can be proposed to explain this point is that the properties of PEO when synthesized inside the IPN may be slightly affected (less entanglement than in the single network for instance).

Concerning the loss factor (tan δ) in the temperature range [−75 to −55 °C], the calculation with Budiansky and $C-L_{PEO}$ expressions are close and fit slightly better than Christensen and Lo prediction with PB as the continuous phase ($C-L_{PB}$). Thus, both the mechanical modelling approach and the experimental approaches [20] confirm that PEO is the continuous phase in 80/20 IPN.

Similar comparisons for low PEO amount (i.e. 20/80 IPN) are presented in Fig. 6. This time Budiansky expression is close to Christensen and Lo prediction with PB as the continuous phase ($C-L_{PB}$) and allows fitting 20/80 IPN modulus. In other words, when one phase is in low concentration in the blend, Budiansky model is equivalent to a 3-phase approach assuming that the continuous matrix is the phase present in large amount. Nevertheless, for this composition, the three models fail to fit the loss factor data. Calculations have been performed on all the other compositions. If one only considers modulus prediction, it may be concluded that the macroscopic continuity seems to be ensured by PB phase for all compositions except 80/20 PEO/PB IPN. However, as the loss factor curves are never accurately fit, except for 80/20 PEO/PB IPN, this conclusion may be hazardous. Thus unfortunately, mechanical modelling of the DMA results is not accurate enough to conclude about phase continuity in the whole series of IPNs. In the following the $LiClO_4$ uptake measurements will help to clarify this point.

3.2. IPN morphology investigation through $LiClO_4$ loading

It has been well established, through solid electrolyte polymer studies [21] that loading a PEO network with $LiClO_4$ noticeably increases its glass transition temperature through physical cross-linking. This particular property can be taken advantage of in the morphology analysis of PEO/PB IPNs. Indeed the addition of $LiClO_4$ to the IPN might lead to a full separation of the relaxation signals of the two combined networks thus leading to a better insight of its morphology.

Thus each IPN film is swollen in an aqueous 1 mol L^{-1} $LiClO_4$ solution at room temperature for the particular length of time which leads to the maximum $LiClO_4$ uptake. In other words each network can be considered as being in its ''salt saturated'' state.

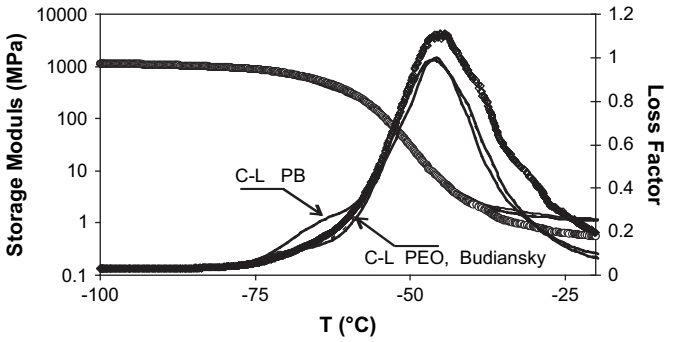

Fig. 5. G' and tan δ versus temperature for (80/20) IPN: experimental data (dots); calculations: normal line: Christensen and Lo with PEO as continuous phase, bold line: Christensen and Lo expression with PB as continuous phase, dotted line: Budiansky model.

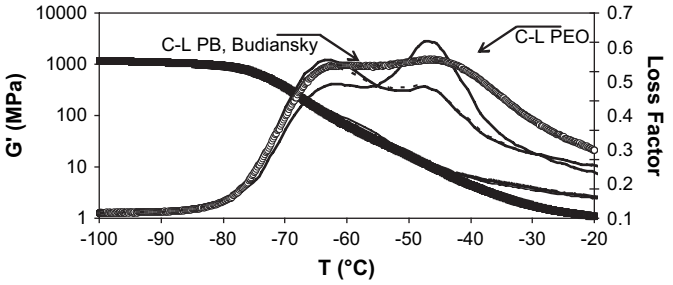

Fig. 6. G' and tan δ versus temperature for (20/80) IPN: experimental data (dots); calculations: normal line: Christensen and Lo with PEO as continuous phase, bold line: Christensen and Lo expression with PB as continuous phase, dotted line: Budiansky model.

The $LiClO_4$ uptake (wt%) and the $[Li^+]/[-CH_2-CH_2-O-]$ or $[Li^+]/[EO]$ ratio are plotted as a function of the PEO weight proportion in the IPN (Fig. 7). As far as single networks are concerned and not surprisingly, $LiClO_4$ does not penetrate the PB single network. On the other hand, due to the strong Li^+–EO interactions, a $LiClO_4$ uptake as high as 25 wt% is achieved for the PEO single network. As far as the IPNs are concerned, the $LiClO_4$ uptake in the films increases with increasing PEO weight proportion. As shown in Fig. 7, the $LiClO_4$ uptake is proportional to the PEO weight proportion between 40 and 100 wt%, the $r = [Li^+]/[-CH_2-CH_2-O]$ ratio remaining almost constant ($r = 0.13$) in this given interval. These results suggest that whatever be the PEO relative weight proportion in the IPN between 40 and 100 wt%, all PEO domains are available for $LiClO_4$ insertion with a constant molar proportion with respect to that of ethylene oxide units. Indeed, these results might be considered as a strong indication of PEO phase continuity in those IPNs. Below 40 wt% PEO in the IPNs, a sharp decrease in the $LiClO_4$ uptake is observed indicating that the insertion of lithium perchlorate is considerably hindered. The $[Li^+]/[-CH_2-CH_2-O]$ ratio decreases sharply from $r = 0.13$ to $r = 0.02$. So, between 10 and 40 wt% PEO, the PB phase is presumed to be continuous in space the PEO domains being less and less interconnected with decreasing PEO weight proportion. Thus, the relative $LiClO_4$ uptake can be related to the extent of accessible PEO and it can be used as a probe for IPN morphology especially.

As it has been pointed out the $LiClO_4$ uptake is likely to alter the mechanical behaviour of the IPNs through selective interaction with the PEO phase. Consequently in order to check this assumption a new IPN mechanical study – using tensile mode solicitation – was then initiated with a given $LiClO_4$ loaded 50/50 IPN and compared with its unloaded counterpart (Fig. 8). The PB α relaxation at -64 °C is unaffected by $LiClO_4$ loading and the PEO α relaxation is shifted from -44 °C to -13 °C. The initially broad tan δ signal characteristic of the unloaded IPN is now nicely split up. Now if the whole $LiClO_4$ loaded PEO/PB IPN series (10–90 wt% PEO composition) is examined as shown in Fig. 9, loss factors are split up in at least two distinct contributions. Thus bearing in mind the fact that PEO and PB relaxations in the corresponding unloaded IPN series occur at close temperature values (in Fig. 2) $LiClO_4$ loading will lead to the possibility

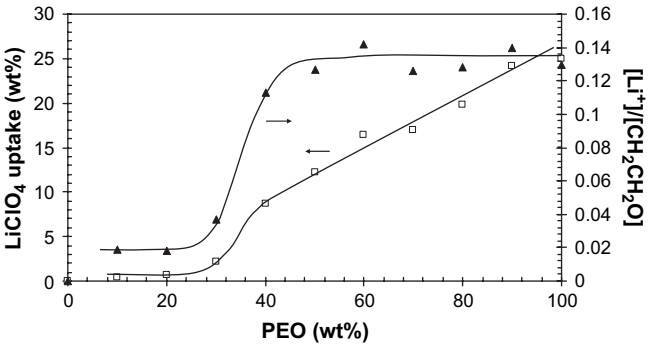

Fig. 7. $LiClO_4$ uptake and Li^+/EO ratio versus PEO content.

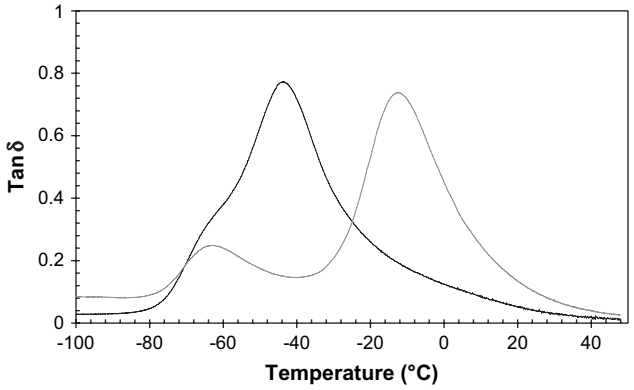

Fig. 8. Loss factor (tan δ) versus temperature for (50/50) PEO/PB IPNs. Black: without $LiClO_4$, gray: with $LiClO_4$ (measured at 1 Hz).

of a finer interpretation of the IPN morphologies as shown in the following part.

In the complete $LiClO_4$ loaded PEO/PB IPN series thermomechanical analysis (Fig. 9) the peak at -64 °C can unambiguously be assigned to the PB phase relaxation and its position shows dependence neither on the weight composition of the IPNs nor on the presence of salt. At temperatures above -50 °C the IPN mechanical spectra are more complex and will be analyzed in two steps with regard to the PEO relative weight proportion: first in the 50–90 wt% PEO range and second in the 40–10 wt% PEO composition bearing in mind that the 50/50 proportion corresponds from mechanical modelling to the phase inversion predicted from Budiansky model.

First in the 50–90 wt% PEO composition range, the $[Li^+]/[CH_2-CH_2-O-]$ ratio remains constant and equal to 0.13, which corresponds to a constant physical cross-linking density. The T_α values vary from -13 °C to 17 °C and are assigned accordingly to the appearance of a PEO/$LiClO_4$ phase (Table 1). In the same composition range IPNs turn from transparent (50/50) to opaque (90/10). This observation together with the T_α set of data witnesses a poorer domain dispersion as the PEO content increases reaching even a coarse morphology in the case of the last sample (90/10).

Furthermore due to $LiClO_4$ loading of the IPN, the PEO/$LiClO_4$ and PB α relaxations remain well separated (T_α

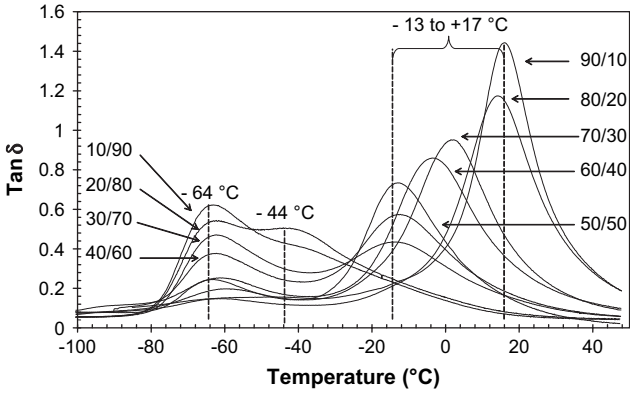

Fig. 9. Loss factor (tan δ) versus temperature for $LiClO_4$ loaded (X/100–X) PEO/PB IPNs (measured at 1 Hz).

Table 1
T_α values for IPNs containing 50–90 wt% PEO

(PEO/PB) IPN weight composition	50/50	60/40	70/30	80/20	90/10
T_α of PEO/$LiClO_4$ phase (°C)	−13	−3	3	15	17

difference of at least 51 °C increasing up to 81 °C) and tan δ values remain equal to less than 0.2 at −44 °C. The absence of any signal at −44 °C indicates that a pure PEO phase is hardly present and that most of the PEO phase can be penetrated by lithium cations. These results are in agreement with $LiClO_4$ uptake experiments, i.e. with the assumption of PEO phase continuity (at least connectivity between PEO domains).

Second, the 40–10 wt% PEO decreasing composition range in the IPNs is examined, i.e. the range where the $[Li^+]/[CH_2-CH_2-O-]$ ratio decreases from 0.13 to 0.02, corresponding to a decreasing physical cross-linking density. A relaxation signal appears around −44 °C which undoubtedly belongs to a PEO fraction unaffected by $LiClO_4$ (Fig. 2). In this composition range the PEO tan δ magnitude at −44 °C increases from 0.2 to 0.45 whereas the PEO/$LiClO_4$ phase relaxation intensity decreases and ultimately disappears for (20/80) and (10/90) IPNs. Taking into account both the $LiClO_4$ uptake curve (Fig. 7) and the DMA curves of the loaded samples (Fig. 9) the 30/70 and 40/60 IPNs can be thus described as three component systems: (i) a PB phase (−64 °C) (ii) a PEO phase at −44 °C (tan $\delta = 0.20$ and 0.24, respectively) and (iii) a PEO/$LiClO_4$ phase (T_α around −14 °C). On the other hand, 10/90 and 20/80 IPNs can be described as two component systems: a PEO phase displaying the typical PEO $T_\alpha = -44$ °C and dispersed in a PB matrix.

The shift from a two phase to a three phase system can be clearly visualized by the fact that the series of unloaded IPN DMA curves show a peculiar point at −54 °C witnessing the presence of two distinct phases whereas the $LiClO_4$ loaded sample curves lead to several intersections located at different temperature values, corresponding to different phases.

Finally, as a sum up of the mechanical studies performed on $LiClO_4$ loaded IPNs the following points can be stressed. The results suggest that the PEO network exists as a continuous phase in the IPNs if the PEO weight proportion is higher than 40 wt%. For composition range between 40 and 10 wt%, PEO domains become more and more disconnected until they are totally isolated from each other. These results are in very good agreement with the $LiClO_4$ uptake measurements.

In the whole PEO composition range IPNs the main T_α transition of the PB phase remains almost constant. Both because of the strong chemical incompatibility of PEO and PB and the fact that all types of analysis [20] showed that PB remains the continuous phase throughout the composition range one can understand that the PB T_α cannot be affected by PEO nodules.

4. Conclusion

In the present paper, the dynamic mechanical properties of interpenetrating polymer networks (IPNs) from hydroxytelechelic polybutadiene and poly(ethylene oxide) are investigated in relation with PB and PEO compositions. Due to the close relaxation temperatures of PEO and PB single networks, the discussion of DMA experimental results on the full IPN composition range is not straight forward. In such a case, the comparison of experimental DMA data with results obtained from mechanical modelling seemed an interesting strategy in order to get some indication on the IPN morphology. However, the mechanical modelling investigation (especially that of the loss factor) of the whole series of IPNs enlightens the fact that this approach is perhaps not as satisfactory to describe IPNs architectures as blends and composites.

On the other hand $LiClO_4$ uptake and DMA measurements performed on $LiClO_4$ loaded IPNs proved more interesting leading to a much finer analysis. Indeed the splitting of the DMA curve clearly indicates the presence of two or three phases in the material depending on the PEO weight proportion: one PB phase and two PEO phases, one of which is loaded with Li^+ cations. According to the same experiments the PEO phase is continuous in space if the PEO weight proportion is higher than 40 wt%. As a result for IPN morphology, dual-phase continuity can be considered in this composition range. Below 40 wt%, PEO phases dispersed in a continuous PB network should be considered.

Specific interactions of PEO and Li^+ cations thus appear to be an interesting and powerful tool, although indirect, to study the morphology in such systems. The specific modification of one property of one selected partner in an IPN architecture could then be considered as a general way of getting a better insight into the morphology of any system where the properties of the two partners are too close to be precisely analyzed.

Acknowledgments

The authors would like to thank Caroline Miro and Marie-Emilie Rebattu for torsion mode mechanical analysis. This work has been supported by the French Ministry of Research (Action Concertée Incitative: MUSARIP).

References

[1] Sperling LH, Klempner D, Utracki LA, editors. Interpenetrating polymer networks. Washington: American Chemical Society; 1994.
[2] Sperling LH, Mishra V. In: Kim SC, Sperling LH, editors. IPNs around the world: science and engineering. New York: Wiley; 1997. p. 1–25.
[3] Sperling LH, editor. Interpenetrating network and related materials. New York: Plenum Press; 1981.
[4] Klempner D, Berkowski L. Interpenetrating polymer networks. In: Kroschwitz JL, editor. Encyclopedia of polymer science and engineering, vol. 8. New York: Wiley; 1987. p. 279–341.
[5] Klempner D, Frisch KC, editors. Polymer alloys II. Polymer science and technology. New York: Plenum Press; 1980.
[6] Millar JR. J Chem Soc 1960:1311–7.
[7] Millar JR. J Chem Soc 1962:1789–94.
[8] Ngai KL, Rizos AK. Macromolecules 1994;27:4493–7.
[9] Alegria A, Colmenero J, Ngai KL, Roland CM. Macromolecules 1994;27:4486–92.
[10] Lipatov Y, Rosovitsky VF, Babkina NV. Polymer 1993;34(22): 4697–702.
[11] Eklind H, Maurer FH, Steeman PAM. Polymer 1997;38:1047–55.

[12] Roland CM, Santangelo PS, Baram Z, Rut J. Macromolecules 1994;27:5382–6.
[13] Georgoussis G, Kyritsis A, Bershtein VA, Fainleib AM, Pissis P. J Polym Sci Part B Polym Phys 2000;38:3070–87.
[14] Cuesta Arenas JM, Mano JF, Gomez Ribelles JL. J Non-cryst Solids 2002;758:307–10.
[15] Widmaier JM, Yeo JK, Sperling LH. Colloid and Polymer Sci 1982;260:678–84.
[16] Hou X, Siow KS. Polymer 2001;42:4181–8.
[17] Hou X, Siow KS. Solid State Ionics 2002;147(3,4):391–5.
[18] Vidal F, Plesse C, Teyssié D, Chevrot C. Synth Met 2004;142: 287–91.
[19] Plesse C, Vidal F, Randriamahazaka H, Teyssié D, Chevrot C. Polymer 2005;46:7771–8.
[20] Plesse C, Vidal F, Gauthier C, Pelletier JM, Teyssié D, Chevrot C. Polymer 2007;48:696–703.
[21] James DB, Wetton RE, Brown DS. Polymer 1979;20(2):187–95.
[22] Hashin ZZ. J Appl Mech 1983;50:481–505.
[23] Takayanagi M, Uemura S, Minami S. J Polym Sci Part C 1964;5:113–22.
[24] Christensen RM, Lo KH. J Mech Phys Solids 1979;27:315–30.
[25] Hervé E, Zaoui A. Int J Eng Sci 1993;31:1–10.
[26] Budiansky B. J Mech Phys Solids 1965;13:223–7.
[27] Chazeau L, Gauthier C, Vigier G, Cavaillé JY. Relationships between microstructural aspects and mechanical properties of polymer-based nanocomposites. In: Nalwa HS, editor. Hybrid materials. Handbook of organic–inorganic hybrid materials and nanocomposites, vol. 1; 2003.
[28] Chabert E, Dendievel R, Gauthier C, Cavaillé JY. Compos Sci Technol 2004;64:309–16.